Available online at www.sciencedirect.com
SCIENCE DIRECT®
Computers and Structures 82 (2004) 1685–1693
Computers & Structures
www.elsevier.com/locate/compstruc

Finite element analysis of superelastic, large deformation behavior of shape memory alloy helical springs

Yutaka Toi [a,*], Jong-Bin Lee [a], Minoru Taya [b]

[a] Institute of Industrial Science, University of Tokyo, 4-6-1 Komaba, Meguro-ku, Tokyo 153-8505, Japan
[b] Center for Intelligent Materials and Systems, University of Washington, Seattle, WA 98195-2600, USA

Received 31 December 2003; accepted 25 March 2004
Available online 17 June 2004

Abstract

Brinson's one-dimensional constitutive modeling for shape memory alloy (SMA) is extended to consider the asymmetric tensile and compressive behavior as well as the torsional behavior. The incremental finite element method using linear Timoshenko beam elements is formulated by the total Lagrangian approach for the superelastic, large deformation analysis of SMA helical springs. The NiTi helical springs are analyzed and the calculated results are compared with the experimental results to show the validity of the present computational procedure in actual design of SMA actuators.

Keywords: Computational mechanics; Finite element method; Shape memory alloy; Constitutive equation; Superelasticity; Large deformation

1. Introduction

The use of shape memory alloys (abbreviated to SMA) has been growing in recent years. It is expected that computational tool will be used more widely in the design of SMA-based actuators. The shape memory alloy has the superelastic effect as well as the shape memory effect. Brinson [1,2] formulated one-dimensional constitutive equation for SMA and applied it to the finite element analysis. Kawai et al. [3], Trochu and Qian [4], Auricchio and Taylor [5], Keefe et al. [6], Tokuda and Sittner [7], Qidwai and Lagoudas [8] also formulated constitutive equations for SMA and some of them were applied to the finite element analysis of SMA devices. However, the computational method has not yet been established for the superelastic, large deformation analysis of SMA helical springs, which are used and expected as actuator devices [9,10].

Brinson's constitutive equation [1], which is relatively simple and phenomenological, is extended to consider the asymmetric tensile and compressive behavior by using Drucker–Prager equivalent stress as in Auricchio and Taylor [5]. It is also extended to the torsional behavior which governs the deformation of helical springs. The incremental finite element formulation by the total Lagrangian approach [11,12] is carried out for the layered linear Timoshenko beam element [12] equipped with the extended Brinson's constitutive equation. The calculated results for TiNi helical springs under tensile loading and unloading are compared with the experimental results given by the CIMS (Center for Intelligent Materials and Systems) at the University of Washington [13] to show the validity of the present method.

2. Constitutive equation for shape memory alloy

The mechanical property of SMA is schematically shown in Fig. 1 [1]. Fig. 1(a) and (b) are the relation between critical transformation stress and temperature

* Corresponding author. Tel.: +81-3-5452-6178; fax: +81-3-5452-6180.
E-mail address: toi@iis.u-tokyo.ac.jp (Y. Toi).

0045-7949/$ - see front matter
doi:10.1016/j.compstruc.2004.03.025

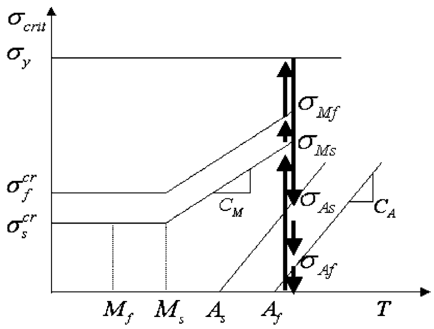

(a) critical stresses for transformation versus temperature

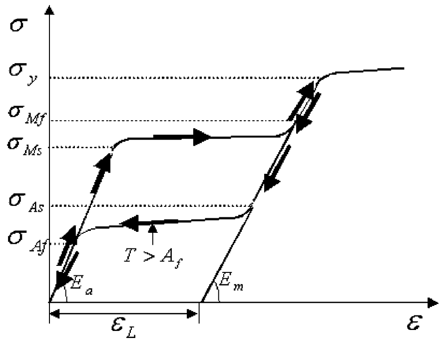

(b) superelastic stress-strain behavior

Fig. 1. Mechanical property of shape memory alloys: (a) critical stresses for transformation versus temperature and (b) superelastic stress–strain behavior.

and the superelastic stress–strain behavior respectively, in which the following symbols are used: T, temperature; σ, stress; ε, strain; $\sigma_{\mathrm{f}}^{\mathrm{cr}}$ and $\sigma_{\mathrm{s}}^{\mathrm{cr}}$, critical finishing and starting stress of martensite transformation; C_{M} and C_{A}, slope for the relation between critical transformation stress and temperature; M_{f} and M_{s}, critical finishing and starting temperature of martensite transformation; A_{s} and A_{f}, critical starting and finishing temperature of austenite transformation. The loading and unloading at the temperature higher than A_{f} occur the superelastic stress–strain behavior as shown in Fig. 1(b).

The one-dimensional stress–strain relation is generally written as

$$\sigma - \sigma_0 = E(\varepsilon - \varepsilon_0) + \Omega(\xi_S - \xi_{S0}) + \theta(T - T_0) \tag{1}$$

where E is the Young's modulus; Ω the transformation coefficient; ξ_S the stress-induced martensite volume fraction, θ the thermal elastic coefficient; T the temperature. The subscript '0' indicates the initial values. Ω is expressed as

$$\Omega = -\varepsilon_L E \tag{2}$$

where ε_L is the maximum residual strain. Young's modulus E is a function of the martensite volume fraction ξ, which is given by

$$E = E_{\mathrm{a}} + \xi(E_{\mathrm{m}} - E_{\mathrm{a}}) \tag{3}$$

where E_{m} and E_{a} are Young's modulus of austenite phase and martensite phase, respectively. The total martensite volume fraction ξ is expressed as

$$\xi = \xi_S + \xi_T \tag{4}$$

where ξ_T is the temperature-induced martensite volume fraction. ξ, ξ_S and ξ_T are functions of the temperature T and the stress σ. To consider the difference between tensile and compressive behavior, von Mises equivalent stress σ_{e} in the evolution equations of ξ, ξ_S and ξ_T is replaced with Drucker–Prager equivalent stress $\sigma_{\mathrm{e}}^{\mathrm{DP}}$ defined as

$$\sigma_{\mathrm{e}}^{\mathrm{DP}} = \sigma_{\mathrm{e}} + 3\beta p \tag{5}$$

where β is the material parameter and p is the hydrostatic pressure given by

$$p = \frac{1}{3}(\sigma_x + \sigma_y + \sigma_z) \tag{6}$$

In one-dimensional case, the equivalent stress in Eq. (5) is expressed as

$$\sigma^{\mathrm{DP}} = |\sigma| + \beta\sigma \tag{7}$$

The effect of using Drucker–Prager equivalent stress instead of von Mises equivalent stress was demonstrated by Toi et al. [9], in which the small deformation, superelastic bending behavior of a Ni–Ti–10%Cu alloy beam subjected to 4-point bending are analyzed by using both Drucker–Prager and von Mises equivalent stress. The stress–strain relations are assumed, based on the tensile test result [5]. The calculated load–displacement curve by using Drucker–Prager equivalent stress, in which $\beta = 0.15$ is assumed, agrees much better with the experimental curve given by Auricchio and Taylor [5] than the result with von Mises equivalent stress.

Substituting Eq. (7) into the evolution equations of ξ, ξ_S and ξ_T given by Brinson [1], the evolution equations for the transformation to martensite phase and austenite phase are expressed as follows:

(i) transformation to martensite phase

$T > M_{\mathrm{s}}$ and $\sigma_{\mathrm{s}}^{\mathrm{cr}}(1+\beta) + C_{\mathrm{M}}(1+\beta)(T - M_{\mathrm{s}}) < \sigma^{\mathrm{DP}} < \sigma_{\mathrm{f}}^{\mathrm{cr}}(1+\beta) + C_{\mathrm{M}}(1+\beta)(T - M_{\mathrm{s}})$:

$$\xi_S = \frac{1-\xi_{S0}}{2}\cos\left\{\frac{\pi}{\sigma_{\mathrm{s}}^{\mathrm{cr}}(1+\beta) - \sigma_{\mathrm{f}}^{\mathrm{cr}}(1+\beta)} \times [\sigma^{\mathrm{DP}} - \sigma_{\mathrm{f}}^{\mathrm{cr}}(1+\beta) - C_{\mathrm{M}}(1+\beta)(T - M_{\mathrm{s}})]\right\} + \frac{1+\xi_{S0}}{2} \tag{8}$$

$$\xi_T = \xi_{T0} - \frac{\xi_{T0}}{1-\xi_{S0}}(\xi_S - \xi_{S0}) \tag{9}$$

$T < M_s$ and $\sigma_s^{cr}(1+\beta) < \sigma^{DP} < \sigma_f^{cr}(1+\beta)$:

$$\xi_S = \frac{1-\xi_{S0}}{2}\cos\left\{\frac{\pi}{\sigma_s^{cr}(1+\beta)-\sigma_f^{cr}(1+\beta)} \times [\sigma^{DP}-\sigma_f^{cr}(1+\beta)]\right\} + \frac{1+\xi_{S0}}{2} \tag{10}$$

$$\xi_T = \xi_{T0} - \frac{\xi_{T0}}{1-\xi_{S0}}(\xi_S - \xi_{S0}) + \Delta_{T\xi} \tag{11}$$

where $M_f < T < M_s$ and $T < T_0$

$$\Delta_{T\xi} = \frac{1-\xi_{T0}}{2}\{\cos[a_M(T-M_f)]+1\} \tag{12}$$

otherwise

$$\Delta_{T\xi} = 0 \tag{13}$$

(ii) transformation to austenite phase

$T > A_s$ and $C_A(1+\beta)(T-A_f) < f < C_A(1+\beta)(T-A_s)$:

$$\xi = \frac{\xi_0}{2}\left\{\cos\left[a_A\left(T - A_s - \frac{f}{C_A(1+\beta)}\right)\right]+1\right\} \tag{14}$$

$$\xi_S = \xi_{S0} - \frac{\xi_{S0}}{\xi_0}(\xi_0 - \xi) \tag{15}$$

$$\xi_T = \xi_{T0} - \frac{\xi_{T0}}{\xi_0}(\xi_0 - \xi) \tag{16}$$

where a_M and a_A are given by the following equations:

$$a_M = \frac{\pi}{M_s - M_f}, \quad a_A = \frac{\pi}{A_f - A_s} \tag{17}$$

It is assumed for simplicity that the superelastic shear deformation behavior is qualitatively similar to the normal deformation behavior and both are independent with each other [14]. The evolution equations for the martensite volume fractions due to the shear stress ξ_τ, $\xi_{S\tau}$ and $\xi_{T\tau}$ are used for the shear deformation. $\sqrt{3}|\tau|$ is employed instead of σ^{DP} in Eq. (7). The shear stress–shear strain relation is expressed by the following equation:

$$\tau - \tau_0 = G(\gamma - \gamma_0) + \Omega_\tau(\xi_{S\tau} - \xi_{S\tau 0}) \tag{18}$$

where G is the shear modulus, Ω_τ the shear transformation constant, $\xi_{S\tau}$; shear stress-induced martensite volume fraction, and T the temperature. The subscript '0' indicates the initial value. Ω_τ is expressed as follows:

$$\Omega_\tau = -\gamma_L G_\tau \tag{19}$$

where γ_L is the maximum residual strain. The shear modulus G is a function of the martensite volume fraction ξ_τ, which is given by

$$G_\tau = G_a + \xi_\tau(G_m - G_a) \tag{20}$$

where G_m and G_a are the elastic shear modulus of martensite phase and austenite phase, respectively. The total martensite volume fraction ξ_τ is expressed as

$$\xi_\tau = \xi_{S\tau} + \xi_{T\tau} \tag{21}$$

where $\xi_{T\tau}$ is the temperature-induced martensite volume fraction. ξ_τ, $\xi_{S\tau}$ and $\xi_{T\tau}$ are functions of the temperature T and the shear stress τ.

$\sqrt{3}|\tau|$ is used as the equivalent stress to express the evolution equations of the martensite volume fractions due to shear, which are given by the following replacements in Eqs. (8)–(17):

$$\begin{gathered} f \to \sqrt{3}|\tau|, \quad \beta = 0, \quad \xi \to \xi_\tau, \quad \xi_0 \to \xi_{\tau 0}, \\ \xi_S \to \xi_{S\tau}, \quad \xi_{S0} \to \xi_{S\tau 0}, \quad \xi_T \to \xi_{T\tau}, \quad \xi_{T0} \to \xi_{T\tau 0}, \\ \Delta_{T\xi} \to \Delta_{T\tau\xi} \end{gathered} \tag{22}$$

3. Finite element formulation

3.1. Incremental constitutive equation

The layered linear Timoshenko beam element [12] as shown in Fig. 2 is used in the finite element analysis of SMA helical springs. The superelastic behavior is assumed for the normal stress (σ)–normal strain (ε) behavior associated with the axial and bending deformation as well as the shear stress (τ)–shear strain (γ) behavior associated with the torsional deformation. The shear deformation associated with the bending deformation is assumed to be elastic and the shear strain energy due to bending is treated as a penalty term because the effect of bending is smaller than torsion in helical springs.

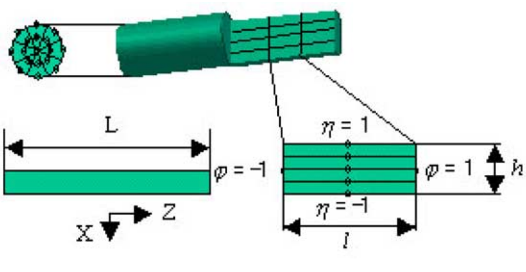

Fig. 2. Layered linear Timoshenko beam element.

The total stress–total strain equations given in Eqs. (1) and (18) are expressed in a differential form as follows:

$$
\begin{aligned}
\mathrm{d}\sigma &= \mathrm{d}E(\varepsilon-\varepsilon_0)+E\mathrm{d}\varepsilon+\mathrm{d}\Omega(\xi_S-\xi_{S0})+\Omega\mathrm{d}\xi_s+\theta\mathrm{d}T\\
&=\frac{\mathrm{d}E}{\mathrm{d}\xi}\left(\frac{\partial\xi}{\partial\sigma}\mathrm{d}\sigma+\frac{\partial\xi}{\partial T}\mathrm{d}T\right)(\varepsilon-\varepsilon_0)+E\mathrm{d}\varepsilon\\
&\quad+\frac{\mathrm{d}\Omega}{\mathrm{d}E}\frac{\mathrm{d}E}{\mathrm{d}\xi}\left(\frac{\partial\xi}{\partial\sigma}\mathrm{d}\sigma+\frac{\partial\xi}{\partial T}\mathrm{d}T\right)(\xi_S-\xi_{S0})\\
&\quad+\Omega\left(\frac{\partial\xi_S}{\partial\sigma}\mathrm{d}\sigma+\frac{\partial\xi_S}{\partial T}\mathrm{d}T\right)+\theta\mathrm{d}T
\end{aligned}\tag{23}
$$

and

$$
\begin{aligned}
\mathrm{d}\tau &= \mathrm{d}G(\gamma-\gamma_0)+G\mathrm{d}\gamma+\mathrm{d}\Omega_\tau(\xi_{S\tau}-\xi_{S\tau0})+\Omega_\tau\mathrm{d}\xi_{S\tau}\\
&=\frac{\mathrm{d}G}{\mathrm{d}\xi_\tau}\left(\frac{\partial\xi_\tau}{\partial\tau}\mathrm{d}\tau+\frac{\partial\xi_\tau}{\partial T}\mathrm{d}T\right)(\gamma-\gamma_0)+G\mathrm{d}\gamma\\
&\quad+\frac{\mathrm{d}\Omega_\tau}{\mathrm{d}G}\frac{\mathrm{d}G}{\mathrm{d}\xi_\tau}\left(\frac{\partial\xi_\tau}{\partial\tau}\mathrm{d}\tau+\frac{\partial\xi_\tau}{\partial T}\mathrm{d}T\right)(\xi_{S\tau}-\xi_{S\tau0})\\
&\quad+\Omega_\tau\left(\frac{\partial\xi_{S\tau}}{\partial\tau}\mathrm{d}\tau+\frac{\partial\xi_{S\tau}}{\partial T}\mathrm{d}T\right)
\end{aligned}\tag{24}
$$

The incremental stress–strain relations are expressed as follows

$$
\begin{aligned}
&\left[1-\frac{\mathrm{d}E}{\mathrm{d}\xi}\frac{\partial\xi}{\partial\sigma}(\varepsilon-\varepsilon_0)-\frac{\mathrm{d}\Omega}{\mathrm{d}E}\frac{\mathrm{d}E}{\mathrm{d}\xi}\frac{\partial\xi}{\partial\sigma}(\xi_S-\xi_{S0})-\Omega\frac{\partial\xi_S}{\partial\sigma}\right]\mathrm{d}\sigma\\
&\quad=E\mathrm{d}\varepsilon+\left[\frac{\mathrm{d}E}{\mathrm{d}\xi}\frac{\partial\xi}{\partial T}(\varepsilon-\varepsilon_0)+\frac{\mathrm{d}\Omega}{\mathrm{d}E}\frac{\mathrm{d}E}{\mathrm{d}\xi}\frac{\partial\xi}{\partial T}(\xi_S-\xi_{S0})\right.\\
&\qquad\left.+\Omega\frac{\partial\xi_S}{\partial T}+\theta\right]\mathrm{d}T
\end{aligned}\tag{25}
$$

and

$$
\begin{aligned}
&\left[1-\frac{\mathrm{d}G}{\mathrm{d}\xi_\tau}\frac{\partial\xi_\tau}{\partial\sigma}(\gamma-\gamma_0)-\frac{\mathrm{d}\Omega_\tau}{\mathrm{d}G}\frac{\mathrm{d}G}{\mathrm{d}\xi_\tau}\frac{\partial\xi_\tau}{\partial\tau}(\xi_{S\tau}-\xi_{S\tau0})\right.\\
&\qquad\left.-\Omega_\tau\frac{\partial\xi_{S\tau}}{\partial\tau}\right]\mathrm{d}\tau\\
&\quad=G\mathrm{d}\gamma+\left[\frac{\mathrm{d}G}{\mathrm{d}\xi_\tau}\frac{\partial\xi_\tau}{\partial T}(\gamma-\gamma_0)+\frac{\mathrm{d}\Omega_\tau}{\mathrm{d}G}\frac{\mathrm{d}G}{\mathrm{d}\xi_\tau}\frac{\partial\xi_\tau}{\partial T}(\xi_{S\tau}-\xi_{S\tau0})\right.\\
&\qquad\left.+\Omega_\tau\frac{\partial\xi_{S\tau}}{\partial T}\right]\mathrm{d}T
\end{aligned}\tag{26}
$$

Therefore the incremental stress–strain relation for the analysis of helical springs is written in the following form:

$$\{\Delta\sigma\}=[D_{\mathrm{se}}](\{\Delta\varepsilon\}-\{\Delta\varepsilon_{\mathrm{se}}\})\tag{27}$$

where

$$
\{\Delta\sigma\}=\begin{Bmatrix}\Delta\sigma\\ \Delta\tau_{xz}\\ \Delta\tau_{yz}\\ \Delta\tau\end{Bmatrix},\quad [D_{\mathrm{se}}]=\begin{bmatrix}E_{\mathrm{se}}&0&0&0\\0&G&0&0\\0&0&G&0\\0&0&0&G_{\mathrm{se}}\end{bmatrix},
$$
$$
\{\Delta\varepsilon\}=\begin{Bmatrix}\Delta\varepsilon\\ \Delta\gamma_{xz}\\ \Delta\gamma_{yz}\\ \Delta\gamma\end{Bmatrix},\quad \{\Delta\varepsilon_{\mathrm{se}}\}=\begin{Bmatrix}\Delta\varepsilon_{\mathrm{se}}\\ 0\\ 0\\ \Delta\gamma_{\mathrm{se}}\end{Bmatrix}\tag{28}
$$

in which τ_{xz} and τ_{yz} (γ_{xz} and γ_{yz}) are the shear stresses (strains) due to bending. The final form of Eq. (27) is given in Refs. [9,10].

3.2. Incremental stiffness equation

The effect of large deformation is taken into account by using the incremental theory by the total Lagrangian approach in which the non-linear terms with respect to the displacement in the axial direction are neglected. The strain increments in the large deformation analysis are given by the following equations [15]:

$$
\begin{aligned}
\Delta\varepsilon&=\frac{\mathrm{d}\Delta\omega}{\mathrm{d}z}-x\frac{\mathrm{d}\Delta\theta_y}{\mathrm{d}z}+y\frac{\mathrm{d}\Delta\theta_x}{\mathrm{d}z}+\frac{\mathrm{d}u}{\mathrm{d}z}\frac{\mathrm{d}\Delta u}{\mathrm{d}z}+\frac{\mathrm{d}v}{\mathrm{d}z}\frac{\mathrm{d}\Delta v}{\mathrm{d}z}\\
&\quad+\frac{1}{2}\left[\left(\frac{\mathrm{d}\Delta u}{\mathrm{d}z}\right)^2+\left(\frac{\mathrm{d}\Delta v}{\mathrm{d}z}\right)^2\right]
\end{aligned}\tag{29}
$$

$$\Delta\gamma_{xz}=\frac{\mathrm{d}\Delta u}{\mathrm{d}z}-\Delta\theta y\tag{30}$$

$$\Delta\gamma_{yz}=\frac{\mathrm{d}\Delta v}{\mathrm{d}z}+\Delta\theta x\tag{31}$$

$$
\begin{aligned}
\Delta\gamma&=\sqrt{x^2+y^2}\frac{\mathrm{d}\Delta\theta_z z}{\mathrm{d}z}-\frac{x}{\sqrt{x^2+y^2}}\frac{\mathrm{d}u}{\mathrm{d}z}\Delta\theta_z\\
&\quad-\frac{x}{\sqrt{x^2+y^2}}\theta_z\frac{\mathrm{d}\Delta u}{\mathrm{d}z}-\frac{y}{\sqrt{x^2+y^2}}\frac{\mathrm{d}v}{\mathrm{d}z}\Delta\theta_z\\
&\quad-\frac{y}{\sqrt{x^2+y^2}}\theta_z\frac{\mathrm{d}\Delta v}{\mathrm{d}z}\frac{x}{\sqrt{x^2+y^2}}\Delta\theta_z\frac{\mathrm{d}\Delta u}{\mathrm{d}z}\\
&\quad-\frac{y}{\sqrt{x^2+y^2}}\Delta\theta_z\frac{\mathrm{d}\Delta v}{\mathrm{d}z}
\end{aligned}\tag{32}
$$

where u, v, w are the translational displacements in the x, y, z-direction, respectively. θ_x, θ_y θ_z are the rotational displacements about the x, y, z-axis, respectively. Then, the incremental relation between strains and nodal displacements is written in a matrix form as follows:

$$\{\Delta\varepsilon\}=[\overline{B}]\{\Delta u\}=([B_0]+[B_L])\{\Delta u\}\tag{33}$$

where the following symbols are used: $[\overline{B}]$; the strain–nodal displacement matrix, $[B_0]$; the strain–nodal displacement matrix without the initial displacements, $[B_L]$; the strain–nodal displacement matrix containing the initial displacements, $\{\Delta u\}$; the nodal displacement increment vector ($\lfloor u \rfloor = \lfloor u_1 v_1 w_1 \theta_{x1} \theta_{y1} \theta_{z1} u_2 v_2 w_2 \theta_{x2} \theta_{y2} \theta_{z2} \rfloor$).

The following element stiffness equation in an incremental form is obtained by the finite element formulation based on the total Lagrangian approach [11,12]:

$$([k_0] + [k_L] + [k_G])\{\Delta u\} = \{\Delta f\} + \{f_{\mathrm{R}}\} + \int_{V_{\mathrm{e}}} [\overline{B}]^{\mathrm{T}} [D] \{\Delta \varepsilon_\theta\} \,\mathrm{d}V^{(0)} \tag{34}$$

where

$$[k_0] = \int_{V_{\mathrm{e}}} [B_0]^{\mathrm{T}} [D] [B_0] \,\mathrm{d}V^{(0)} \tag{35}$$

$$[k_L] = \int_{V_{\mathrm{e}}} ([B_0]^{\mathrm{T}} [D] [B_L] + [B_L]^{\mathrm{T}} [D] [B_0] + [B_L]^{\mathrm{T}} [D] [B_L]) \,\mathrm{d}V^{(0)} \tag{36}$$

$$[k_G] = \int_{V_{\mathrm{e}}} [G]^{\mathrm{T}} [S] [G] \,\mathrm{d}V^{(0)} \tag{37}$$

The following symbols are used: $[k_0]$, the incremental stiffness matrix; $[k_L]$, the initial displacement matrix; $[k_G]$; the initial stress matrix; $\{\Delta f\}$, the external force increment vector; $\{f_R\}$, the unbalanced force vector; $[D_{\mathrm{se}}]$, the superelastic stress–strain matrix; $\{\Delta\varepsilon_{\mathrm{se}}\}$, the superelastic initial strain vector; $[G]$; the gradient matrix; $[S]$, the initial stress matrix and V_{e}, the element volume.

The final forms of the matrices $[B_0]$, $[B_L]$, $[G]$ and $[S]$ for the layered linear Timoshenko beam element are expressed as follows:

$$[B] = \begin{bmatrix} 0 & 0 & -\frac{1}{l} & \frac{b\lambda}{2l} & \frac{h\eta}{2l} & 0 & 0 & 0 & \frac{1}{l} & -\frac{b\lambda}{2l} & -\frac{h\eta}{2l} & 0 \\ -\frac{1}{l} & 0 & 0 & 0 & -\frac{1-\varphi}{2} & 0 & \frac{1}{l} & 0 & 0 & 0 & -\frac{1+\varphi}{2} & 0 \\ 0 & -\frac{1}{l} & 0 & -\frac{1-\varphi}{2} & 0 & 0 & 0 & \frac{1}{l} & 0 & -\frac{1-\varphi}{2} & 0 & 0 \\ 0 & 0 & 0 & 0 & 0 & -\frac{\sqrt{h^2\eta^2+b^2\lambda^2}}{2L} & 0 & 0 & 0 & 0 & 0 & \frac{\sqrt{h^2\eta^2+b^2\lambda^2}}{2l} \end{bmatrix} \tag{38}$$

$$[B_L] = \left[\begin{matrix} \left(\frac{\mathrm{d}N_1}{\mathrm{d}Z}\right)^2 u_1 + \frac{\mathrm{d}N_1}{\mathrm{d}Z}\frac{\mathrm{d}N_2}{\mathrm{d}Z} u_2 & \left(\frac{\mathrm{d}N_1}{\mathrm{d}Z}\right)^2 v_1 + \frac{\mathrm{d}N_1}{\mathrm{d}Z}\frac{\mathrm{d}N_2}{\mathrm{d}Z} v_2 & 0 \\ 0 & 0 & 0 \\ 0 & 0 & 0 \\ -\frac{x}{\sqrt{x^2+y^2}}\left(N_1 \frac{\mathrm{d}N_1}{\mathrm{d}Z}\theta_{Z1} + N_2 \frac{\mathrm{d}N_1}{\mathrm{d}Z}\theta_{Z2}\right) & -\frac{x}{\sqrt{x^2+y^2}}\left(N_1 \frac{\mathrm{d}N_1}{\mathrm{d}Z}\theta_{Z1} + N_2 \frac{\mathrm{d}N_1}{\mathrm{d}Z}\theta_{Z2}\right) & 0 \end{matrix} \right.$$

$$\begin{matrix} 0 & 0 & 0 \\ 0 & 0 & 0 \\ 0 & 0 & 0 \\ 0 & 0 & -\frac{x}{\sqrt{x^2+y^2}} N_1 \frac{\mathrm{d}N_1}{\mathrm{d}Z} u_1 - \frac{y}{\sqrt{x^2+y^2}} N_1 \frac{\mathrm{d}N_1}{\mathrm{d}Z}\frac{\mathrm{d}N_1}{\mathrm{d}Z} v_1 - \frac{x}{\sqrt{x^2+y^2}} N_1 \frac{\mathrm{d}N_2}{\mathrm{d}Z} u_2 - \frac{y}{\sqrt{x^2+y^2}} N_1 \frac{\mathrm{d}N_2}{\mathrm{d}Z} v_2 \end{matrix}$$

$$\begin{matrix} \frac{\mathrm{d}N_1}{\mathrm{d}Z}\frac{\mathrm{d}N_2}{\mathrm{d}Z} u_1 + \left(\frac{\mathrm{d}N_2}{\mathrm{d}Z}\right) u_2 & \frac{\mathrm{d}N_1}{\mathrm{d}Z}\frac{\mathrm{d}N_2}{\mathrm{d}Z} v_1 + \left(\frac{\mathrm{d}N_2}{\mathrm{d}Z}\right) v_2 & 0 \\ 0 & 0 & 0 \\ 0 & 0 & 0 \\ -\frac{x}{\sqrt{x^2+y^2}}\left(N_1 \frac{\mathrm{d}N_2}{\mathrm{d}Z}\theta_{Z1} + N_2 \frac{\mathrm{d}N_2}{\mathrm{d}Z}\theta_{Z2}\right) & -\frac{y}{\sqrt{x^2+y^2}}\left(N_1 \frac{\mathrm{d}N_2}{\mathrm{d}Z}\theta_{Z1} + N_2 \frac{\mathrm{d}N_2}{\mathrm{d}Z}\theta_{Z2}\right) & 0 \end{matrix}$$

$$\left. \begin{matrix} 0 & 0 & 0 \\ 0 & 0 & 0 \\ 0 & 0 & 0 \\ 0 & 0 & -\frac{x}{\sqrt{x^2+y^2}} N_2 \frac{\mathrm{d}N_1}{\mathrm{d}Z} u_1 - \frac{y}{\sqrt{x^2+y^2}} N_2 \frac{\mathrm{d}N_1}{\mathrm{d}Z} v_1 - \frac{x}{\sqrt{x^2+y^2}} N_2 \frac{\mathrm{d}N_2}{\mathrm{d}Z} u_2 - \frac{y}{\sqrt{x^2+y^2}} N_2 \frac{\mathrm{d}N_2}{\mathrm{d}Z} v_2 \end{matrix} \right] \tag{39}$$

$$[S] = \begin{bmatrix} \sigma_Z & 0 & 0 & 0 & 0 & 0 \\ 0 & \sigma_Z & 0 & 0 & 0 & 0 \\ 0 & 0 & 0 & 0 & 0 & -\frac{y}{2\sqrt{x^2+y^2}}\tau_{\theta Z} \\ 0 & 0 & 0 & 0 & \frac{x}{2\sqrt{x^2+y^2}}\tau_{\theta Z} & 0 \\ 0 & 0 & 0 & \frac{x}{2\sqrt{x^2+y^2}}\tau_{\theta Z} & 0 & 0 \\ 0 & 0 & -\frac{y}{2\sqrt{x^2+y^2}}\tau_{\theta Z} & 0 & 0 & 0 \end{bmatrix} \tag{40}$$

$$[G] = \begin{bmatrix} \frac{dN_1}{dZ} & 0 & 0 & 0 & 0 & 0 & \frac{dN_2}{dZ} & 0 & 0 & 0 & 0 & 0 \\ 0 & \frac{dN_1}{dZ} & 0 & 0 & 0 & 0 & 0 & \frac{dN_2}{dZ} & 0 & 0 & 0 & 0 \\ 0 & 0 & 0 & 0 & 0 & N_1 & 0 & 0 & 0 & 0 & 0 & N_2 \\ 0 & 0 & 0 & 0 & 0 & -N_1 & 0 & 0 & 0 & 0 & 0 & -N_2 \\ \frac{dN_1}{dZ} & 0 & 0 & 0 & 0 & -y\frac{dN_1}{dZ} & \frac{dN_2}{dZ} & 0 & 0 & 0 & 0 & -y\frac{dN_2}{dZ} \\ 0 & \frac{dN_1}{dZ} & 0 & 0 & 0 & x\frac{dN_1}{dZ} & 0 & \frac{dN_2}{dZ} & 0 & 0 & 0 & x\frac{dN_2}{dZ} \end{bmatrix} \tag{41}$$

where l, b and h are the length, the width and the depth of the beam element respectively, while φ, η and λ are the corresponding non-dimensional coordinates ($-1 \leqslant \varphi, \eta, \lambda \leqslant 1$). N_1 and N_2 are the shape functions, which are given as follows:

$$N_1 = \frac{1}{2}(1-\varphi), \quad N_2 = \frac{1}{2}(1+\varphi) \tag{42}$$

4. Finite element analysis of SMA helical springs

The finite element formulation described in the preceding chapter has applied to the analysis of the tensile

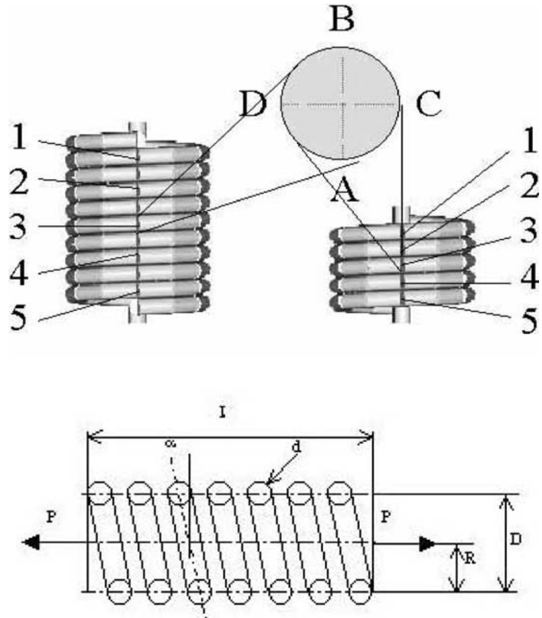

Fig. 3. SMA helical spring.

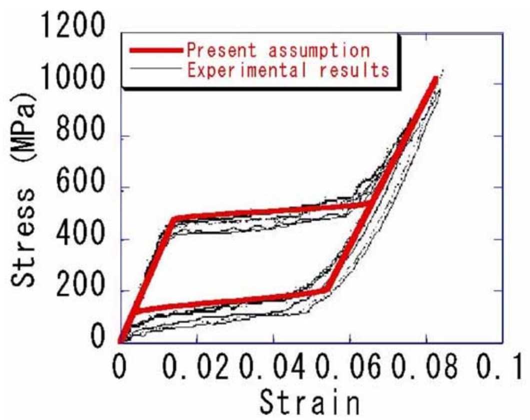

(a) long stroke

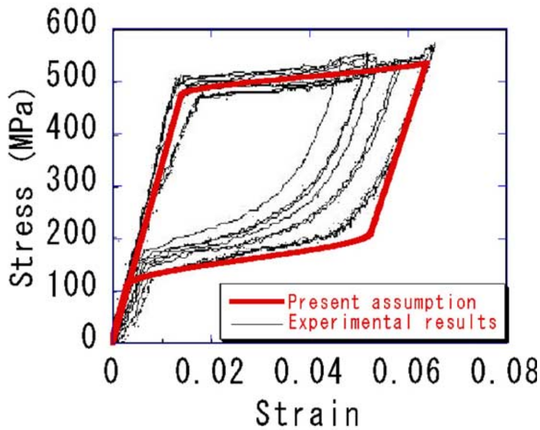

(b) short stroke

Fig. 4. Assumed stress–strain curves: (a) long stroke and (b) short stroke.

Table 1
Dimensions and material constants of NiTi helical springs

Dimensions (mm)	Material constants (MPa)
5 turns	$E_m = 28500$, $E_a = 34000$
$L = 5$ (total length)	$G_m = 10690$, $G_a = 12753$
$d = 1$ (diameter)	$\sigma_{MS} = \sigma_s^{cr} + C_M(T - M_s) = 427.8$
$D = 7.3$ (diameter)	$\sigma_{Mf} = \sigma_f^{cr} + C_M(T - M_s) = 542.8$
	$\sigma_{AS} = C_A(T - A_s) = 210.5$
	$\sigma_{Af} = C_A(T - A_f) = 110.4$
10 turns	$\varepsilon_L = \gamma_L = 0.047$
$L = 10$ (Total length)	$\beta = 0.15$
$d = 1$ (diameter)	
$D = 7.3$ (diameter)	

loading and unloading tests of SMA helical springs conducted at the CIMS of the University of Washington [13]. The numbers of turns of the helical springs tested are 5 and 10 as shown in Fig. 3. Fig. 4 shows the comparison between the experimental and the assumed stress–strain curves for the material of the tested springs subjected to the long and short stroke. The assumed material constants are shown in Table 1. Fig. 5 shows the tensile load–displacement curves for the spring with 5 turns under the stroke of 70 mm and the spring with 10 turns under the stroke of 90 mm. The two springs are subdivided with 64 and 124 elements respectively. The numbers of incremental steps used are so large (1060 and 5500, respectively) that the iteration calculation in each loading step is not done in the present analysis, although the iteration is effective to improve the accuracy and efficiency of the incremental analysis as pointed out by Bathe [12]. The calculated results are in good agreement with the experimental results, however, there is a little difference in the shape of curves, which is mainly caused by the lack of the material test results available under torsion. The calculated stress–strain curves at some sampling points in the spring with 5 turns under some different strokes are shown in Fig. 6. It is seen that the normal stress–normal strain curves are all elastic while

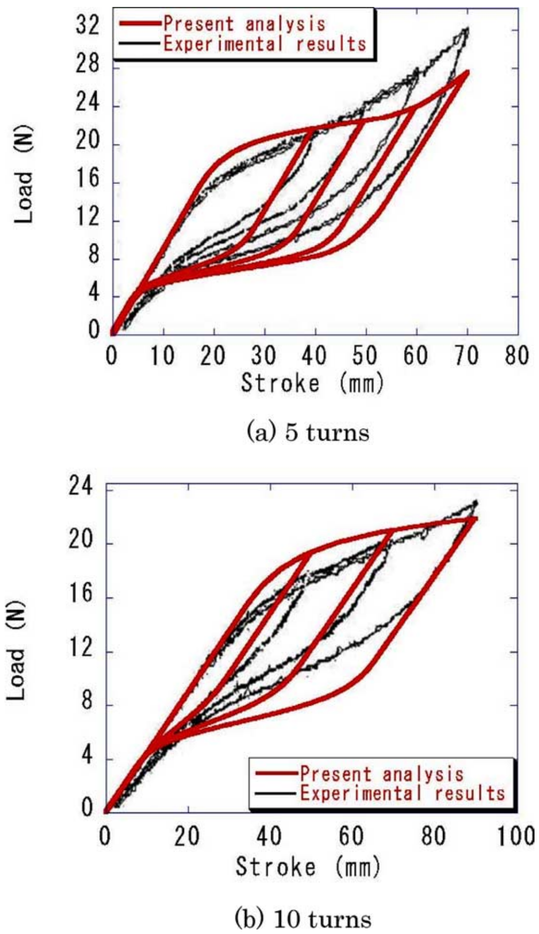

Fig. 5. Calculated load–stroke curves: (a) 5 turns and (b) 10 turns.

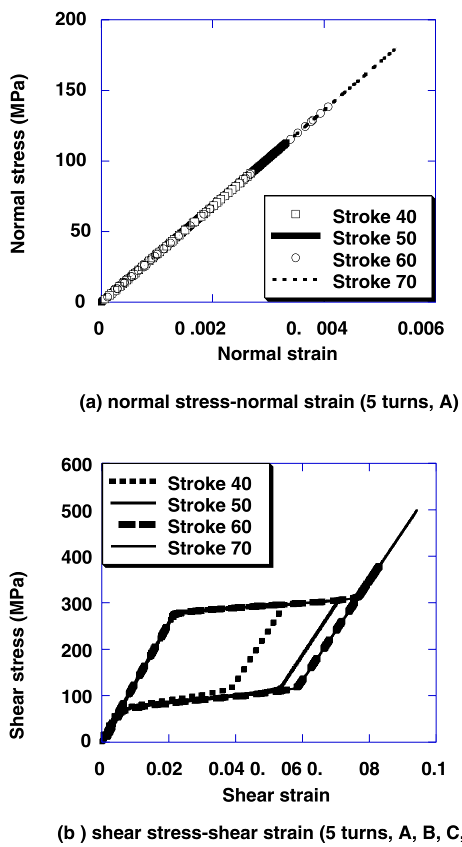

Fig. 6. Calculated stress–strain curves: (a) normal stress–normal strain (5 turns, A) and (b) shear stress–shear strain (5 turns, A–D).

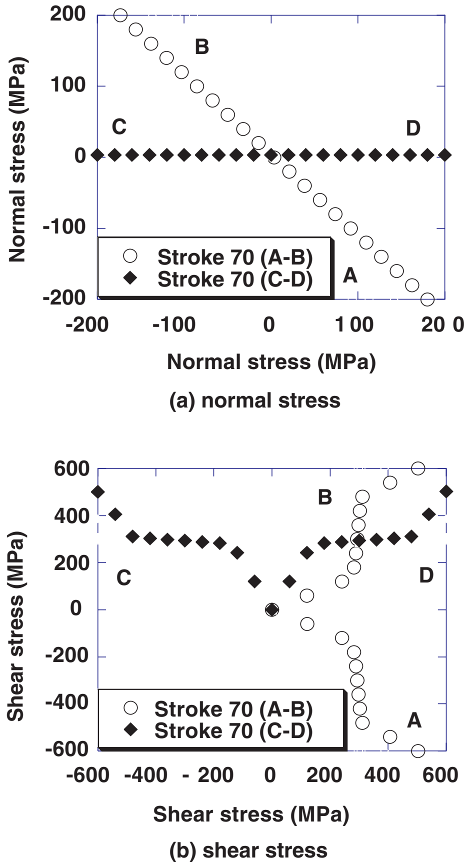

Fig. 7. Calculated stress distributions (5 turns): (a) normal stress and (b) shear stress.

the shear stress–shear strain curve are superelastic, because the torsional shear governs the deformation of helical springs. Fig. 7 shows the distributions of normal and shear stress on the cross-section of the spring with 5 turns, in which the line A–B and C–D are indicated in Fig. 3.

5. Concluding remarks

The finite element formulation has been presented for the analysis of superelastic behaviors of SMA helical spring in the present study. Brinson's one-dimensional constitutive modeling for SMA has been extended to consider the asymmetric tensile and compressive behavior and the torsional deformation. The incremental finite element analysis program has been developed by using the layered linear Timoshenko beam element equipped with the extended Brinson's constitutive modeling for SMA.

The developed program has applied to the superelastic, large deformation analysis of TiNi helical springs under tensile loading and unloading. The calculated results have been compared with the test results given by the CIMS at the University of Washington. The calculated results have corresponded well with the experimental results. The material test results under torsion and the consideration of coupling of the superelastic behaviors under tension–compression and torsion are necessary in order to obtain improved results. The extension to the coupled magneto-superelastic analysis of ferromagnetic SMA such as FePd is now under way [16].

References

[1] Brinson LC. One-dimensional constitutive behavior of shape memory alloy: thermomechanical derivation with non-constant material functions and redefined martensite internal variable. J Intell Mater Syst Struct 1993;4:229–42.
[2] Brinson LC, Lammering R. Finite element analysis of the behavior of shape memory alloys and their applications. Int J Solids Struct 1993;30(23):3261–80.
[3] Kawai M, Ogawa H, Baburaj V, Koga T. A phenomenological multiaxial constitutive model for shape memory alloys and its application (Part 1: report, comparison between multiaxial formulations and an extension to TiNi-SMA model). Tans Jpn Soc Mech Eng (A) 1997;63(615): 3751–8 [in Japanese].
[4] Trochu F, Qian YY. Nonlinear finite element simulation of superelastic shape memory alloy parts. Comput Struct 1997;62(5):799–810.
[5] Auricchio F, Taylor RL. Shape memory alloy: modeling and numerical simulations of the finite-strain superelastic behavior. Comput Methods Appl Mech Eng 1997;143:175–94.
[6] Keefe AC, Carman GP, Jardine AP. Torsional behavior of shape memory alloys. In: SPIE Conference on Smart Materials Technologies; 1998. p. 58–67.
[7] Tokuda M, Sittner P. Multi-axial constitutive equations for polycrystalline shape memory alloy (1st report, modeling and formulation). Trans Jpn Soc Mech Eng (A) 1999;65(631):491–7 [in Japanese].
[8] Qidwai MA, Lagoudas DC. Numerical implementation of a shape memory alloy thermomechanical constitutive model using return mapping algorithims. Int J Numer Methods Eng 2000;47:1123–68.
[9] Toi Y, Lee JB, Taya, M, Finite element analysis of superelastic behavior of shape memory alloy devices (part 1: small deformation analysis of tensile and bending behaviors). Trans Jpn Soc Mech Eng (A) 2002;68(676): 1688–94 [in Japanese].
[10] Toi Y, Lee JB, Taya, M, Finite element analysis of superelastic behavior of shape memory alloy devices (part 2: finite deformation analysis of beams and helical springs). Trans Jpn Soc Mech Eng (A) 2002;68(676):1695–701 [in Japanese].
[11] Washizu K. Variational methods in elasticity and plasticity. 3rd ed. Oxford: Pergamon Press; 1982.

[12] Bathe KJ. Finite element procedures. Englewood Cliffs, NJ: Prentice Hall; 1996.
[13] Toi Y, Lee JB, Taya M, Matsunaga Y, Finite element analysis of superelastic, large-deformation behavior of shape memory alloy helical springs, Seisan-Kenkyu [Bimonthly report of the Institute of Industrial Science, University of Tokyo] 2002;54(5):339–42 [in Japanese].
[14] Sun QP, Li ZQ. Phase transformation in superelastic NiTi polycrystalline micro-tubes under tension and torsion: from localization to homogeneous deformation. Int J Solids Struct 2002;39:3797–809.
[15] Kawai T. Analysis of buckling problems. Baihukan; 1974 [in Japanese].
[16] Toi Y, Lee JB, Taya M. Coupled magneto-superelastic analysis of ferromagnetic shape memory alloy helical springs. Seisan-Kenkyu (Bimonthly report of the Institute of Industrial Science, University of Tokyo) 2003;55(5): 453–6.